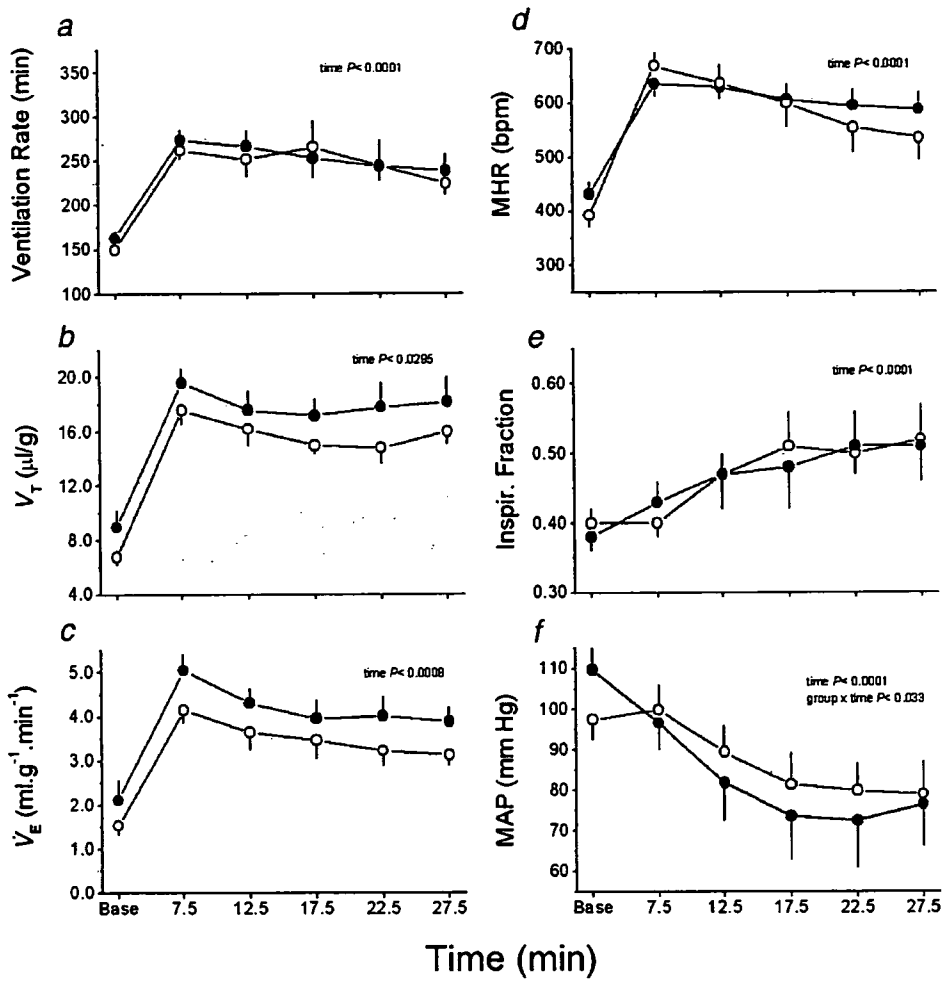

Fig. 3 Mean values of haemodynamic and ventilatory functions (±SEM) during exposure to acute hypoxia (10% O_2) after i.p. pretreatment with idazoxan in WT (*open symbols*) and PGID (*closed symbols*) mice. Mean values of 5-min intervals are presented in relation to median time

sympathoinhibition of HR when hypoxia is sustained. In rodents, a sustained increase in pulmonary arterial pressure occurs during hypoxia [39]. Increased lung inflation and pulmonary blood flow stimulate pulmonary vagal afferent C-fibres, leading to central sympathoinhibition [5]. Therefore, a decline in mechanoreceptor stimulation and a sustained increase in C-fibre stimulation would both act to cause sympathoinhibition. The extent to which the latter potentiates the HR decline remains to be determined.

Pathways influencing cardiac premotor neurones

The NTS integrates afferent information from the peripheral chemoreceptors, baroreceptors and pulmonary mechanoreceptors and together with the surrounding nuclei in the medulla, pons and hypothalamus (defense area) directly modulate the activity of bulbospinal neurones [40]. Premotor neurones within the rostral ventrolateral medulla (RVLM) are considered to be sympathoexcitatory as direct stimulation evokes HR increase and the release of catecholamines. Furthermore, both carotid body chemoreceptor and hypothalamic stimulation augment RVLM neural activity [40, 41]. Inhibition or destruction of RVLM neurones results in the loss of cardiovascular defense responses [40]. Since sympathetic neural discharge shows clear respiratory entrainment that is related to the increase in firing rate of noradrenergic neurones of the pons during hypoxia, it was suggested that RVLM activation of these nuclei in the pons might directly modify vasomotor and cardiac outflows in a respiratory dependent manner [42].

Role for α_2-AR in coupling HR responses to inspiration during the chemoreflex

α_2-AR are present on a large fraction of bulbospinal presympathetic motor neurones [43, 44], including the central serotonergic neurons [7], the spinal and intracardiac ganglia, and the atria [45, 46]. Many researchers have independently shown that presynaptic α_2-AR are an important regulator of central NA release [8–11, 47]. To investigate the role of α_2-AR in the regulation of HR during acute hypoxia, we used pretreatment with the partially selective antagonist idazoxan. At high doses (5 mg/kg or more) idazoxan was shown to reduce 5-HT

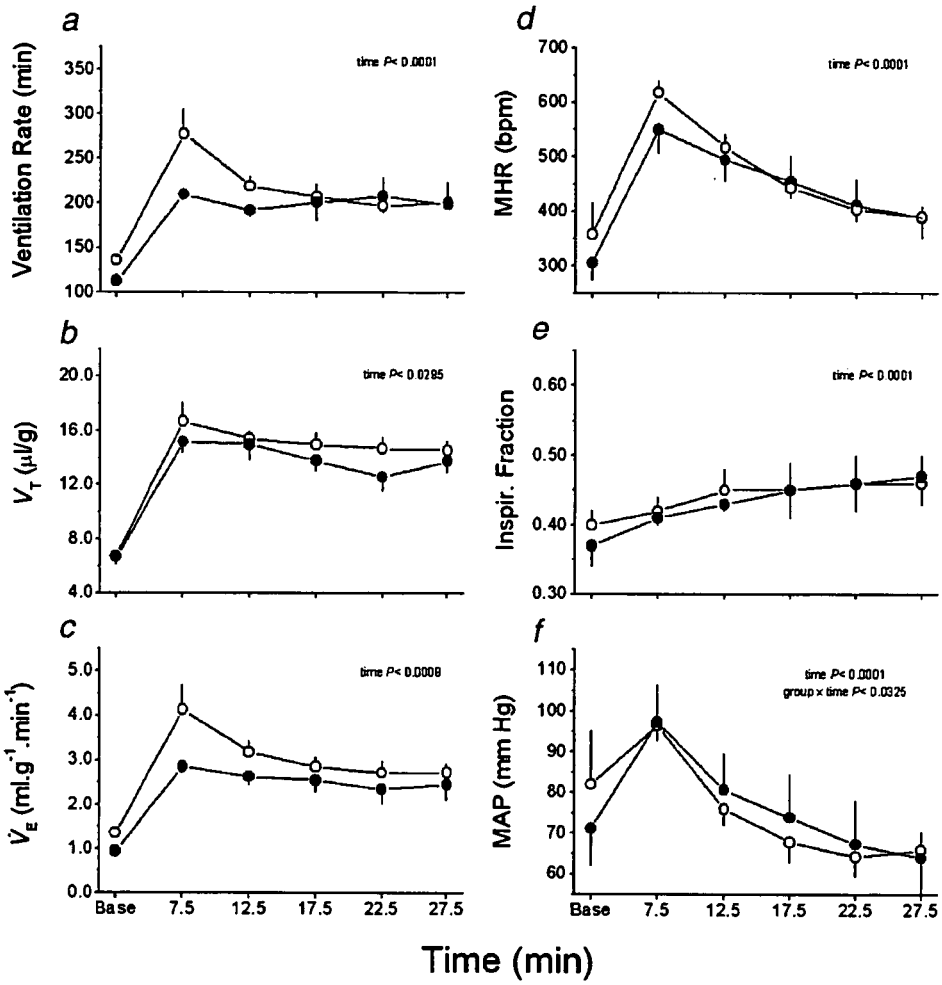

Fig. 4 Mean values of haemodynamic and ventilatory functions (±SEM) during exposure to acute hypoxia (10% O_2) after i.p. pretreatment with sodium meclofenamate in WT (*open symbols*) and PGID (*closed symbols*) mice. Mean values of 5-min intervals are presented in relation to median time

synthesis by its agonistic actions on 5-HT_{1A} autoreceptors in the brains of conscious rats [48], but not at lower doses [47, 48]. In fact, most selective α_2-AR antagonists were shown to also act as agonists on 5-HT_{1A} autoreceptors on the serotonergic neurons at high doses [49]. In this study however, idazoxan at a dose of 3 mg/kg i.p. is unlikely to have caused increased activation of 5-HT_{1A} and an increase in reflex vagal activity as it resulted in an increase in HR under the normoxic baseline and potentiated the HR response throughout hypoxia (Figs. 3 and 5). Further, Skinner et al. [50] demonstrated that the activation of central 5-HT_{1A} receptors via the stimulation of cardiopulmonary afferents results in a vagal bradycardia that is attenuated with a selective 5-HT_{1A} antagonist. However, they were unable to demonstrate a similar role for 5-HT_{1A} in the peripheral chemoreflex. Others have also recently suggested that endogenous activation of central 5-HT_{1A} does not play an important role in some stress responses involving sympathoactivation [51].

On the other hand, sympathetic innervation of the carotid body elicits an inhibitory effect on carotid chemoreceptor responses to sustained hypoxia that is largely mediated by α_2-AR [12]. Thus, a negative feedback mechanism is likely to contribute to the secondary decline in ventilation and MHR during hypoxia observed in this study. Since idazoxan enhanced cardiac sympathoactivation in this study, it is likely that a significant amount of secondary HR reduction during sustained hypoxia is facilitated by α_2-AR mediated attenuation of sympathoactivation of the cardiac premotor neurones. It still remains to be determined whether this α_2-AR mediated sympathoinhibition is primarily a central or peripheral effect. Furthermore, while idazoxan did not stimulate 5-HT_{1A} mediated bradycardia, we cannot rule out the likely possibility that hypoxic activation of α_2-AR by endogenous NA in untreated mice simultaneously facilitates parasympathetic-mediated HR reductions. The α_2-AR agonist clonidine was shown not only to cause sympathoinhibition, but also to activate vagal activity [52, 53].

Do PG modulate acute cardiorespiratory responses to hypoxia in mice?

Receptors for both PGI_2 and PGE_2 are distributed in unique regions of the brainstem important for cardiovascular reflex

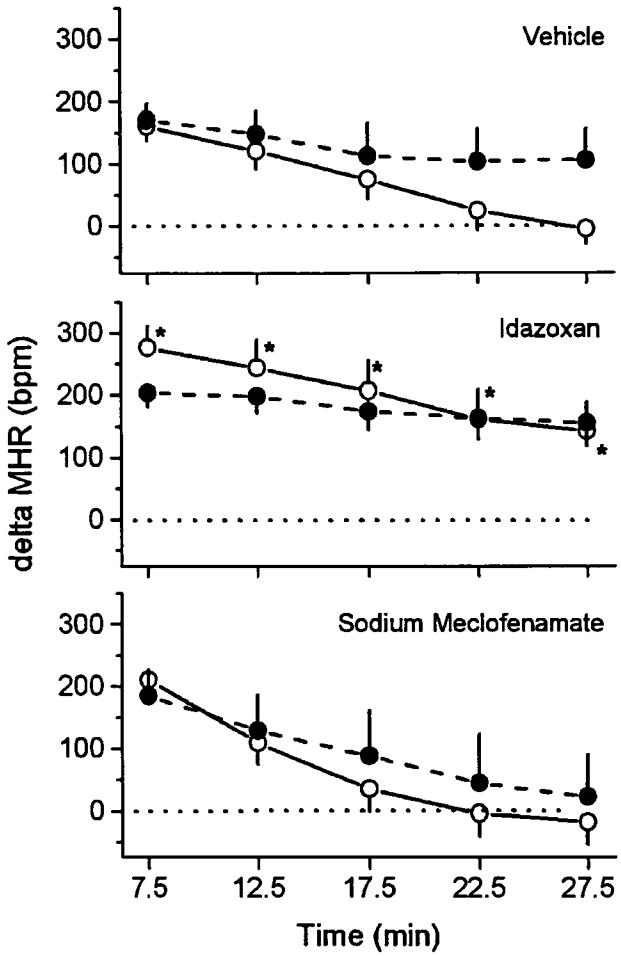

Fig. 5 Effects of vehicle, idazoxan and sodium meclofenamate i.p. pretreatment on delta MHR (±SEM) response to acute hypoxia exposure in WT (*open symbols*) and PGID (*closed symbols*) mice. Idazoxan increased the hypoxic MHR change (relative to resting normoxia baseline) of WT mice, but not in PGID mice. No significant difference was found by ANOVA between groups for either treatment. *$p<0.05$ vs vehicle response

regulation [21], but the roles of these PGs within the CNS are poorly understood. In the periphery, both PGs are important inhibitors of sympathetic activity to the carotid body and the heart, and therefore might modulate the peripheral chemoreflex. In rabbits, PGE_2 is an important inhibitor of increased catecholamine release from carotid chemoreceptors during hypoxia [22]. In PGID mice, both PGE_2 and thromboxane are elevated several times above WT basal levels [23]. Based on past studies, elevated basal levels of PGE_2 would be predicted to attenuate the hypoxic ventilatory response [22, 54], not potentiate it as seen in PGID mice. Therefore, we can only conclude that the hypoxic ventilatory responses of these mice might have been potentiated to compensate for exaggerated pulmonary vasoconstriction with elevated thromboxane expression since sodium meclofenamate eliminated ventilatory differences from WT (Fig. 4). Alternatively, an unknown cyclooxygenase product might evoke the opposite effect to PGE_2 on chemoreceptor activity as first speculated by Gomez-Nino et al. based on their detailed studies [22]. Hence, it is not possible to conclude from our findings in this study, in the absence of studies on other PG, whether PGI_2 mediated attenuation of sympathoactivation is mediated by its actions on carotid chemoreceptor activity. Nevertheless, the hypoxic ventilatory responses of mice in this study are consistent with a role for α_2-AR mediated inhibition of carotid body activity [12, 55].

Two findings suggest that PGI_2 acts to increase cardiac chemosensitivity by lowering the threshold of excitability of neural pathways regulating sympathetic cardiac premotor neurones. First, in a normoxic environment, HR was not elevated after idazoxan treatment in WT mice with endogenous PGI_2 present. Second, under conditions of sympathoactivation, the size of the hypoxic HR response was diminished in PGID mice (Fig. 5). The former indicates that PGI_2 by itself is sufficient to reduce basal sympathetic cardiac efferent activity when central outflow is increased by idazoxan [8, 9]. Both catecholamines and increased HR cause increased release of PGI_2 from the pericardium and epicardium, which is thought to inhibit neural activity of the postganglionic fibres as they pass through the pericardial space [56, 57]. Finally, hypoxic HR was increased in excess of that expected on the basis of increased inspiratory flow in WT mice only, probably because PGI_2 lowered the threshold for sympathoactivation. Here, we assume that thromboxane or a PG other than PGI_2 is responsible for the elevated inspiratory flow in vehicle treated PGID mice during sustained hypoxia. This PG product is therefore also likely to be responsible for the sustained elevation of MHR of up to 100 bpm above that of vehicle treated WT mice during the sustained hypoxic

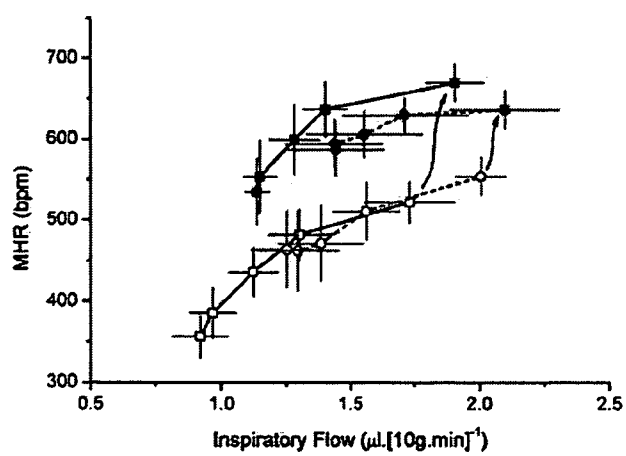

Fig. 6 Temporal changes in the relation between inspiratory flow and hypoxic MHR after vehicle (*open symbols*) and idazoxan (*closed symbols*) pretreatments in WT (*squares*) and PGID (*circles*) mice. Group mean±SEM are presented for the 5-min intervals during hypoxia from Figs. 2 and 3. *Arrows* indicate the shift in peak MHR response (5–10 min) between vehicle and idazoxan treatments

exposure (30 min). PGI_2 is widely believed to be the most important PG vasodilator released by the endothelium of the coronary vascular bed during hypoxia and ischaemia [14–16, 18, 19] and the pericardium itself [57] during sympathoactivation. Several decades earlier, it was shown that PGI_2 attenuated the tachycardia evoked by hypoxia by increasing the effectiveness of an α_2-AR feedback mechanism in the spinal ganglia [14, 16]. Taken together, these studies all suggest that PGI_2 is an important part of the feedback mechanism regulating sympathoactivation during sustained hypoxia in the conscious animal. Similar roles for PGI_2 in the central sensitization of pain and immune responses are well-known [58].

Future research needs to clarify if there is a role for PGI_2 in the modulation of the afferent pathways of the peripheral chemoreflex. It is noteworthy that receptors for PGI_2 are found in both vagal and sympathetic afferent fibres (nodose and dorsal root ganglia) [21, 59]. It still remains to be determined whether the observed effects of PGI_2 on chemoreflex responses are modulated by cardiac sympathetic afferent activity or by enhancing the effectiveness of α_2-AR mediated inhibition at the carotid body. We conclude that α_2-AR play an important role in preventing overactivation of cardiac sympathetic activity during exposure to acute hypoxia in conscious, spontaneously breathing mice. As the central inspiratory drive declines during sustained hypoxia, HR declines secondarily. This study shows that depression of HR in conscious mice not only involves vagal activation, but also has a significant component that is attributed to the reduction of sympathetic outflow to cardiac premotor neurones.

Acknowledgments This work was supported in part by the Promotion of Fundamental Studies in Health Sciences of the Pharmaceuticals and Medical Devices Agency (PDMA) of Japan to K. Kangawa and a Ministerial Grant-in-Aid for Scientific Research to M. Shirai (13670053). We are grateful to T. Ono (Primetech, Osaka) for his technical support.

References

1. Marshall JM (1994) Peripheral chemoreceptors and cardiovascular regulation. Physiol Rev 74:543–594
2. Marshall J, Metcalfe J (1988) Analysis of the cardiovascular changes induced in the rat by graded levels of systemic hypoxia. J Physiol 407:385–403
3. Marshall J, Metcalfe J (1990) Effects of systemic hypoxia on the distribution of cardiac output in the rat. J Physiol 426:335–353
4. Spyer KM (1994) Annual review prize lecture. Central nervous mechanisms contributing to cardiovascular control. J Physiol 474:1–19
5. Daly MD (1991) Some reflex cardioinhibitory responses in the cat and their modulation by central inspiratory neuronal activity. J Physiol 439:559–577
6. Hilaire G, Viemari JC, Coulon P, Simonneau M, Bevengut M (2004) Modulation of the respiratory rhythm generator by the pontine noradrenergic A5 and A6 groups in rodents. Respir Physiol Neurobiol 143:187–197
7. Kinkead R, Bach KB, Johnson SM, Hodgeman BA, Mitchell GS (2001) Plasticity in respiratory motor control: intermittent hypoxia and hypercapnia activate opposing serotonergic and noradrenergic modulatory systems. Comp Biochem Physiol A Mol Integr Physiol 130:207–218
8. Szemeredi K, Komoly S, Kopin IJ, Bagdy G, Keiser HR, Goldstein DS (1991) Simultaneous measurement of plasma and brain extracellular fluid concentrations of catechols after yohimbine administration in rats. Brain Res 542:8–14
9. Gradin K, Nicholas AP, Hjemdahl P, Svensson T, Hokfelt T (1992) Contrasting cardiovascular responses from intrathecal administration of epinephrine and norepinephrine in conscious rats: role of alpha 1- and alpha 2-adrenoceptors. J Cardiovasc Pharmacol 20:367–374
10. Makaritsis KP, Johns C, Gavras I, Altman JD, Handy DE, Bresnahan MR, Gavras H (1999) Sympathoinhibitory function of the $alpha_{2A}$-Adrenergic receptor subtype. Hypertension 34:403–407
11. Guyenet PG (2000) Neural structures that mediate sympathoexcitation during hypoxia. Respir Physiol 121:147–162
12. Prabhakar NR, Kou YR (1994) Inhibitory sympathetic action on the carotid body responses to sustained hypoxia. Respir Physiol 95:67–79
13. Gonzales R, Sherbourne CD, Goldyne ME, Levine JD (1991) Noradrenaline-induced prostaglandin production by sympathetic postganglionic neurons is mediated by $alpha_2$-Adrenergic receptors. J Neurochem 57:1145–1150
14. Wennmalm M, FitzGerald GA, Wennmalm A (1987) Prostacyclin as neuromodulator in the sympathetically stimulated rabbit heart. Prostaglandins 33:675–691
15. de Deckere EA, Nugteren DH, Ten Hoor F (1977) Prostacyclin is the major prostaglandin released from the isolated perfused rabbit and rat heart. Nature 268:160–163
16. Edlund A, Fredholm BB, Patrignani P, Patrono C, Wennmalm A, Wennmalm M (1983) Release of two vasodilators, adenosine and prostacyclin, from isolated rabbit hearts during controlled hypoxia. J Physiol 340:487–501
17. Schror K, Funke K (1985) Prostaglandins and myocardial noradrenaline overflow after sympathetic nerve stimulation during ischemia and reperfusion. J Cardiovasc Pharmacol 7:S50–S54
18. Woditsch I, Schror K (1992) Prostacyclin rather than endogenous nitric oxide is a tissue protective factor in myocardial ischemia. Am J Physiol 263:H1390–H1396
19. Godecke A, Decking UKM, Ding Z, Hirchenhain J, Bidmon HJ, Godecke S, Schrader J (1998) Coronary hemodynamics in endothelial NO synthase knockout mice. Circ Res 82:186–194
20. Longhurst JC, Tjen-A-Looi SC, Fu LW (2001) Cardiac sympathetic afferent activation provoked by myocardial ischemia and reperfusion: mechanisms and reflexes. Ann N Y Acad Sci 940:74–95
21. Matsumura K, Watanabe Y, Onoe H (1995) Prostacyclin receptor in the brain and central terminals of the primary sensory neurons: an autoradiographic study using a stable prostacyclin analogue [^{3}H]iloprost. Neuroscience 65:493–503
22. Gomez-Nino A, Almaraz L, Gonzalez C (1994) In vitro activation of cyclo-oxygenase in the rabbit carotid body: effect of its blockade on [^{3}H]catecholamine release. J Physiol 476:257–267
23. Yokoyama C, Yabuki T, Shimonishi M, Wada M, Hatae T, Ohkawara S, Takeda J, Kinoshita T, Okabe M, Tanabe T (2002) Prostacyclin-deficient mice develop ischemic renal disorders including nephrosclerosis and renal infarction. Circulation 106:2397–2403
24. Butz GM, Davisson RL (2001) Long-term telemetric measurement of cardiovascular parameters in awake mice: a physiological genomics tool. Physiol Genomics 5:89–97

25. Drorbaugh JE, Fenn WO (1955) A barometric method for measuring ventilation in newborn infants. Pediatrics 16:81–87
26. Withers PC (1977) Measurement of VO_2, VCO_2, and evaporative water loss with a flow-through mask. J Appl Physiol 42:120–123
27. Antier D, Franconi F, Sannajust F (1999) Idazoxan does not prevent but worsens focal hypoxic-ischemic brain damage in neonatal Wistar rats. J Neurosci Res 58:690–696
28. Vayssettes-Courchay C, Bouysset F, Cordi AA, Laubie M, Verbeuren TJ (1996) A comparative study of the reversal by different alpha2-adrenoceptor antagonists of the central sympatho-inhibitory effect of clonidine. Br J Pharmacol 117:587–593
29. Gonzalez JD, Llinas MT, Nava E, Ghiadoni L, Salazar FJ (1998) Role of nitric oxide and prostaglandins in the long-term control of renal function. Hypertension 32:33–38
30. Llinas MT, Lopez R, Rodriguez F, Roig F, Salazar FJ (2001) Role of COX-2-derived metabolites in regulation of the renal hemodynamic response to norepinephrine. Am J Physiol Renal Physiol 281:F975–F982
31. Walker BR, Voelkel NF, Reeves JT (1982) Pulmonary pressor response after prostaglandin synthesis inhibition in conscious dogs. J Appl Physiol 52:705–709
32. Murata T, Ushikubi F, Matsuoka T, Hirata M, Yamasaki A, Sugimoto Y, Ichikawa A, Aze Y, Tanaka T, Yoshida N, Ueno A, Oh-ishi S, Narumiya S (1997) Altered pain perception and inflammatory response in mice lacking prostacyclin receptor. Nature 388:678–682
33. Hoshikawa Y, Voelkel NF, Gesell TL, Moore MD, Morris KG, Alger LA, Narumiya S, Geraci MW (2001) Prostacyclin receptor-dependent modulation of pulmonary vascular remodeling. Am J Respir Crit Care Med 164:314–318
34. Gautier H, Bonora M (1992) Ventilatory and metabolic responses to cold and hypoxia in intact and carotid body-denervated rats. J Appl Physiol 73:847–854
35. Nakano H, Lee SD, Ray AD, Krasney JA, Farkas GA (2001) Role of nitric oxide in thermoregulation and hypoxic ventilatory response in obese Zucker rats. Am J Respir Crit Care Med 164:437–442
36. Thomas T, Marshall JM (1994) Interdependence of respiratory and cardiovascular changes induced by systemic hypoxia in the rat: the roles of adenosine. J Physiol 480:627–636
37. Guyenet PG (1997) Is the hypotensive effect of clonidine and related drugs due to imidazoline binding sites? Am J Physiol 273: R1580–R1584
38. Downing S, Mitchell J, Wallace A (1963) Cardiovascular responses to ischemia, hypoxia, and hypercapnia of the central nervous system. Am J Physiol 204:881–887
39. Schwenke DO, Pearson JT, Mori H, Shirai M (2006) Does central nitric oxide elicit pulmonary hypertension in conscious rats? Respir Physiol Neurobiol (in press). DOI 10.1016/j.resp.2005.12.002
40. Dampney RA (1994) Functional organization of central pathways regulating the cardiovascular system. Physiol Rev 74:323–364
41. Fontes MA, Tagawa T, Polson JW, Cavanagh SJ, Dampney RA (2001) Descending pathways mediating cardiovascular response from dorsomedial hypothalamic nucleus. Am J Physiol Heart Circ Physiol 280:H2891–H2901
42. Guyenet PG, Koshiya N, Huangfu D, Verberne AJ, Riley TA (1993) Central respiratory control of A5 and A6 pontine noradrenergic neurons. Am J Physiol 264:R1035–R1044
43. Rosin DL, Zeng D, Stornetta RL, Norton FR, Riley T, Okusa MD, Guyenet PG, Lynch KR (1993) Immunohistochemical localization of alpha 2A-adrenergic receptors in catecholaminergic and other brainstem neurons in the rat. Neuroscience 56: 139–155
44. Guyenet PG, Stornetta RL, Riley T, Norton FR, Rosin DL, Lynch KR (1994) Alpha2A-adrenergic receptors are present in lower brainstem catecholaminergic and serotonergic neurons innervating spinal cord. Brain Res 638:285–294
45. Brodde OE, Michel MC (1999) Adrenergic and muscarinic receptors in the human heart. Pharmacol Rev 51:651–690
46. Brum PC, Kosek J, Patterson A, Bernstein D, Kobilka B (2002) Abnormal cardiac function associated with sympathetic nervous system hyperactivity in mice. Am J Physiol Heart Circ Physiol 283:H1838–H1845
47. Pifl C, Pichler L, Kobinger W, Hornykiewicz O (1988) The dopamine autoreceptor agonist, B-HT 920, preferentially reduces brain dopamine release in vivo: biochemical indices of brain dopamine, noradrenaline and serotonin in ventriculocisternal perfusates in the cat. Eur J Pharmacol 153:33–44
48. Llado J, Esteban S, Garcia-Sevilla JA (1996) The alpha 2-adrenoceptor antagonist idazoxan is an agonist at 5-HT1A autoreceptors modulating serotonin synthesis in the rat brain in vivo. Neurosci Lett 218:111–114
49. McCall RB, Harris LT, King KA (1991) Sympatholytic action of yohimbine mediated by 5-HT1A receptors. Eur J Pharmacol 199:263–265
50. Skinner MR, Ramage AG, Jordan D (2002) Modulation of reflexly evoked vagal bradycardias by central 5-HT_{1A} receptors in anaesthetized rabbits. Br J Pharmacol 137:861–873
51. Nalivaiko E, Ootsuka Y, Blessing WW (2005) Activation of 5-HT1A receptors in the medullary raphe reduces cardiovascular changes elicited by acute psychological and inflammatory stresses in rabbits. Am J Physiol Regul Integr Comp Physiol 289:R596–R604
52. Godwin SJ, Tortelli CF, Parkin ML, Head GA (1998) Comparison of the baroreceptor-heart rate reflex effects of moxonidine, rilmenidine and clonidine in conscious rabbits. J Auton Nerv Syst 72:195–204
53. Tank J, Jordan J, Diedrich A, Obst M, Plehm R, Luft FC, Gross V (2004) Clonidine improves spontaneous baroreflex sensitivity in conscious mice through parasympathetic activation. Hypertension 43:1042–1047
54. Gonzalez C, Almaraz L, Obeso A, Rigual R (1994) Carotid body chemoreceptors: from natural stimuli to sensory discharges. Physiol Rev 74:829–898
55. Kou YR, Ernsberger P, Cragg PA, Cherniack NS, Prabhakar NR (1991) Role of alpha 2-adrenergic receptors in the carotid body response to isocapnic hypoxia. Respir Physiol 83:353–364
56. Dusting GJ, Nolan RD (1981) Stimulation of prostacyclin release from the epicardium of anaesthetized dogs. Br J Pharmacol 74:553–562
57. Miyazaki T, Pride HP, Zipes DP (1990) Prostaglandins in the pericardial fluid modulate neural regulation of cardiac electrophysiological properties. Circ Res 66:163–175
58. Tilley SL, Coffman TM, Koller BH (2001) Mixed messages: modulation of inflammation and immune responses by prostaglandins and thromboxanes. J Clin Invest 108:15–23
59. Nakae K, Hayashi F, Hayashi M, Yamamoto N, Iino T, Yoshikawa S, Gupta J (2005) Functional role of prostacyclin receptor in rat dorsal root ganglion neurons. Neurosci Lett 388:132–137

Available online at www.sciencedirect.com
ScienceDirect
Journal of Molecular and Cellular Cardiology 42 (2007) 88–97
Journal of Molecular and Cellular Cardiology
www.elsevier.com/locate/yjmcc

Original article

Transplantation of mesenchymal stem cells attenuates myocardial injury and dysfunction in a rat model of acute myocarditis

Shunsuke Ohnishi [a,*,1], Bobby Yanagawa [a,1], Koichi Tanaka [a], Yoshinori Miyahara [a], Hiroaki Obata [a,b], Masaharu Kataoka [a], Makoto Kodama [b], Hatsue Ishibashi-Ueda [c], Kenji Kangawa [d], Soichiro Kitamura [e], Noritoshi Nagaya [a,*]

[a] *Department of Regenerative Medicine and Tissue Engineering, National Cardiovascular Center Research Institute, Fujishirodai 5-7-1, Osaka 565-8565, Japan*
[b] *Division of Cardiology, Niigata University Graduate School of Medical and Dental Sciences, Niigata, Japan*
[c] *Department of Pathology, National Cardiovascular Center, Osaka, Japan*
[d] *Department of Biochemistry, National Cardiovascular Center Research Institute, Osaka, Japan*
[e] *Department of Cardiovascular Surgery, National Cardiovascular Center, Osaka, Japan*

Received 11 May 2006; received in revised form 29 August 2006; accepted 2 October 2006
Available online 13 November 2006

Abstract

Acute myocarditis is a non-ischemic inflammatory disease of the myocardium for which there is currently no specific treatment. We have previously shown that mesenchymal stem cells (MSC) can ameliorate heart injury during acute ischemia and in dilated cardiomyopathy; however, the therapeutic potential in acute myocarditis is unclear. In this study, we investigated the ability of MSC to attenuate myocardial injury and dysfunction during the acute phase of experimental myocarditis. Ten-week-old male Lewis rats were injected with porcine myosin to induce myocarditis. Cultured MSC (3×10^6 cells/rat) were injected intravenously 7 days after myosin injection. At 3 weeks, myosin injection resulted in severe inflammation and significant deterioration of cardiac function. MSC transplantation attenuated increases in CD68-positive inflammatory cells and monocyte chemoattractant protein-1 (MCP-1) expression in myocardium, and improved cardiac function in this model. Furthermore, myocardial capillary density was higher in myocarditis tissue, and was further increased by MSC transplantation. *In vitro*, cultured adult rat cardiomyocytes were injured in response to MCP-1, whereas this effect was attenuated by MSC-derived conditioned medium, suggesting cardioprotective effects of MSC acting in a paracrine manner. MSC transplantation attenuated myocardial injury and dysfunction in a rat model of acute myocarditis, at least in part through paracrine effects of MSC.

Keywords: Acute myocarditis; Mesenchymal stem cell; Paracrine effect; Cytokine; Cell death

1. Introduction

Acute myocarditis is a non-ischemic heart disease characterized by myocardial inflammation and edema. This disease is associated with rapidly progressive heart failure, arrhythmias and sudden death [1,2]. Although the early evidence for efficacy of immunoglobulin and interferon therapy appears promising, these results have yet to be demonstrated in randomized or controlled clinical trials. The current options are restricted to supportive care for heart failure or arrhythmias. The lack of specific treatment and the potential severity of the illness emphasize the importance of novel and effective therapeutic strategies for myocarditis.

Mesenchymal stem cells (MSC) are multipotent stem cells present in adult tissues, and have the ability to differentiate into a variety of lineages, including vascular smooth muscle cells, endothelial cells and cardiomyocytes [3,4]. We have previously reported that bone marrow-derived MSC engrafted in experimental myocardial infarction expressed both cardiac and endothelial phenotypes in the heart, and further increased capillary density and decreased the infarct size [5]. Moreover, we have recently demonstrated that monolayered MSC derived from adipose tissue reversed wall thinning in the scar area and improved cardiac function in rats with myocardial infarction [6]. The cardioprotective effects of MSC are known to be mediated

* Corresponding authors. Tel.: +81 6 6833 5012; fax: +81 6 6833 9865.
E-mail addresses: sonsihi@ri.ncvc.go.jp (S. Ohnishi), nnagaya@ri.ncvc.go.jp (N. Nagaya).
[1] Drs Ohnishi and Yanagawa contributed equally to this study.

0022-2828/$ - see front matter © 2006 Elsevier Inc. All rights reserved.
doi:10.1016/j.yjmcc.2006.10.003

not only by their differentiation into vascular cells and cardiomyocytes, but also by their ability to supply large amounts of angiogenic, anti-apoptotic and mitogenic factors [5–7]. These findings suggest the therapeutic potential of MSC for heart failure. However, whether intravenously transplanted MSC attenuate myocardial inflammation and cardiac dysfunction in acute myocarditis remains unknown.

In the present study, we used porcine myosin-induced acute myocarditis in Lewis rats. This model closely resembles human giant cell myocarditis, a frequently fatal disorder characterized by multinucleated giant cells in the myocardium [8]. To examine the therapeutic potential of MSC in the acute phase of myocarditis, MSC were intravenously injected into rats 7 days after myosin injection.

Thus, the purposes of this study were 1) to investigate whether intravenous transplantation of MSC improves cardiac function and pathological findings including myocardial inflammation in rats with myosin-induced myocarditis, and 2) to investigate the underlying mechanisms responsible for the effects of MSC.

2. Materials and methods

2.1. Animals

Ten-week-old male Lewis rats (Japan SLC, Hamamatsu, Japan) were used in all experiments, and were maintained in our animal facilities. The experimental protocols were approved by The Animal Care Committee of the National Cardiovascular Center.

2.2. Preparation of cardiac myosin

Purified cardiac myosin from the ventricular muscle of pig hearts was prepared according to a procedure described previously [8]. The antigen was dissolved at a concentration of 20 mg/ml in phosphate-buffered saline (PBS) containing 0.3 M KCl, mixed with an equal volume of complete Freund's adjuvant containing 11 mg/ml *Mycobacterium tuberculosis* (Difco Laboratories, Sparks, MD, USA). Rats were anesthetized with an intraperitoneal injection of 20 mg/kg sodium pentobarbital, and 0.1 ml of the antigen-adjuvant emulsion was injected into the each footpad.

2.3. Acute myocarditis model

Forty-five rats were randomly divided into three groups and received the following treatment: 1) 0.2 ml saline and sham surgery (Sham group, $n=15$), 2) 0.2 ml cardiac myosin antigen and sham surgery (MyoC group, $n=15$), and 3) 0.2 ml cardiac myosin followed by MSC transplantation 7 days post-myosin injection (MyoC+MSC group, $n=15$). Rats were weighed and observed daily for signs of morbidity and for death.

2.4. Preparation and transplantation of bone marrow-derived MSC

MSC were prepared as described previously [5]. Briefly, bone marrow cells were isolated by flushing out the femoral and tibial cavities with PBS, and plated onto 10-cm dishes in complete culture medium: Dulbecco's Modified Eagle's Medium (DMEM), 15% fetal bovine serum, 100 U/ml penicillin and 100 μg/ml streptomycin. Five days after plating, non-adherent cells were removed, and adherent cells were further propagated for 4 to 5 passages.

Seven days after myosin injection, MSC (3×10^6 cells) or vehicle (0.9% saline) was intravenously administered via the jugular vein. Sham rats also received saline administration but without myosin injection.

2.5. Hemodynamic studies

Hemodynamic studies were performed on day 21 post-myosin injection. Anesthesia was maintained with an intraperitoneal injection of 20 mg/kg sodium pentobarbital, and a 1.5 Fr micromanometer-tipped catheter was placed in the left ventricle through the right carotid artery (Millar Instruments, Houston, TX, USA). Heart rate (HR) was also monitored by electrocardiography. HR, mean arterial pressure (MAP), left ventricular systolic pressure (LVSP), left ventricular end-diastolic pressure (LVEDP), maximum dP/dt (Max dP/dt) and minimum dP/dt (Min dP/dt) were used as indices of hemodynamics, and recorded simultaneously during ventilation after a minimum equilibration period of 20 min.

2.6. Echocardiographic studies

Echocardiography was performed on day 21 post-myosin injection. Rats were anesthetized with an intraperitoneal injection of 20 mg/kg sodium pentobarbital. A 12 MHz probe was placed at the left 4th intercostal space for M-mode imaging using 2D echocardiography (Sonos 5500, Philips, Bothell, WA, USA). Left ventricular systolic dimension (LVDs), left ventricular diastolic dimension (LVDd), anterior wall thickness (AWT), posterior wall thickness (PWT) and ejection fraction (EF) were measured, and taken as an average of three beats. Fractional shortening (%FS) was calculated as $(LVDd-LVDs)/LVDd\times100$.

2.7. Histological examination

The heart was excised above the origin of the great vessels, and heart weight and body weight were recorded on day 21 post-myosin injection. Portions of the midventricular heart, spleen, pancreas, kidney and liver were fixed with 4% paraformaldehyde, embedded in paraffin, sectioned at 4-μm thickness, stained with either hematoxylin and eosin (H & E) or Masson's trichrome, and subjected to immunohistochemical staining. H & E-stained sections were evaluated by a cardiovascular pathologist (H.I.-U.) for the characterization of myocardial injury and inflammation without knowledge of the experimental groups, on the following scale: 0, absent or questionable presence; 1, limited focal distribution; 2–3, intermediate severity; and 4, coalescent and extensive foci throughout the entire transversely sectioned ventricular tissue.

2.8. Immunohistochemical study

Paraffin-embedded heart sections were washed in increasing concentrations of ethanol and then with PBS. Sections were incubated with Protein Block (DakoCytomation, Glostrup, Denmark), then with mouse anti-rat von Willebrand Factor (vWF) (DakoCytomation), CD68 (DakoCytomation) or monocyte chemoattractant protein-1 (MCP-1) (BD Biosciences Pharmingen, San Jose, CA, USA) antibody in diluent for 40 min, followed by incubation with horseradish peroxidase (HRP)-linked rabbit anti-mouse IgG (DakoCytomation) for 30 min. Sections were visualized using 0.5% diaminobenzidine and 0.03% hydrogen peroxide, and counterstained with hematoxylin. The numbers of CD68-stained cells and vWF-stained capillaries were determined in 10 randomly selected fields (×200).

2.9. Enzyme-linked immunosorbent assay (ELISA)

Serum MCP-1 level of rats on day 21 post-myosin injection was measured using a Rat MCP-1 ELISA kit (Biosource International, Carmarillo, CA, USA). Vascular endothelial growth factor (VEGF) and hepatocyte growth factor (HGF) levels in the supernatant of MSC culture (2.3×10^5 cells in 10-cm dish cultured for 48 h) were measured using ELISA kits, according to the manufacturers' protocols (HGF, Institute of Immunology, Tokyo, Japan; VEGF, R&D Systems, Minneapolis, MN, USA).

2.10. Isolation of cardiomyocytes

Ventricular cardiomyocytes were obtained as described previously with modification [9]. Briefly, after heparinization by intraperitoneal injection of 1000 U/kg heparin sodium, the heart was rapidly excised, and pulmonary, connective and other noncardiac tissues were removed. The heart was then mounted on the cannula of a modified Langendorff apparatus and perfused with buffer containing 0.75 mg/ml collagenase type I (Worthington, Lakewood, NJ, USA), 0.5 mg/ml hyaluronidase (Sigma) and 1% bovine serum albumin (fraction V, ICN, Aurora, OH, USA), in a recirculating fashion for 3 h. After the perfusion sequence, the heart was removed from the perfusion apparatus, the atrium was removed, and gently minced. The enzyme-containing buffer was harvested and the cardiomyocytes resuspended in fresh buffer. The calcium concentration in the suspension was raised stepwise to 1.2 mM. Quiescent, calcium-tolerant cardiomyocytes were gravitationally separated from any nonventricular cells and resuspended in complete culture medium. The culture medium was exchanged for fresh medium to remove the damaged myocytes that failed to attach 3 h after plating. After this procedure, 80% to 90% myocytes were viable and showed rod-shape.

2.11. Cardiomyocyte stimulation and MTS assay

To assess cardioprotective effects of MSC acting in a paracrine manner, we investigated whether conditioned medium obtained from MSC culture attenuated MCP-1-induced cardiomyocyte injury. Cardiomyocytes were plated on 96-well plates (1×10^3 viable cells/well) precoated with laminin (BD Biosciences Pharmingen). After 3 h, the medium was changed to fresh DMEM containing 15% FBS or conditioned medium obtained from MSC culture, with or without 50 ng/ml MCP-1 (R&D Systems, Minneapolis, MN, USA). After 24 h, the cellular level of 3-(4,5-dimethylthiazol-2-yl)-5-(3-carboxymethoxyphenyl)-2-(4-sulfophenyl)-2H-tetrazolium (MTS), indicative of the mitochondrial function in living cells and cell viability, was measured ($n=6$) with a CellTiter96 AQueous One Kit (Promega, Madison, WI, USA) and a Microplate Reader (490 nm, Bio-Rad, Hercules, CA, USA).

2.12. In vitro apoptosis assay

Terminal dUTP nick end labeling (TUNEL) assay (ApopTag Fluorescein In Situ Apoptosis Detection Kit, Chemicon International, Temecula, CA, USA) was performed to evaluate apoptosis of cultured cardiomyocytes. After incubation for 24 h, cardiomyocytes were fixed in 1% paraformaldehyde, and TUNEL staining was performed for detection of apoptotic nuclei according to the manufacturer's

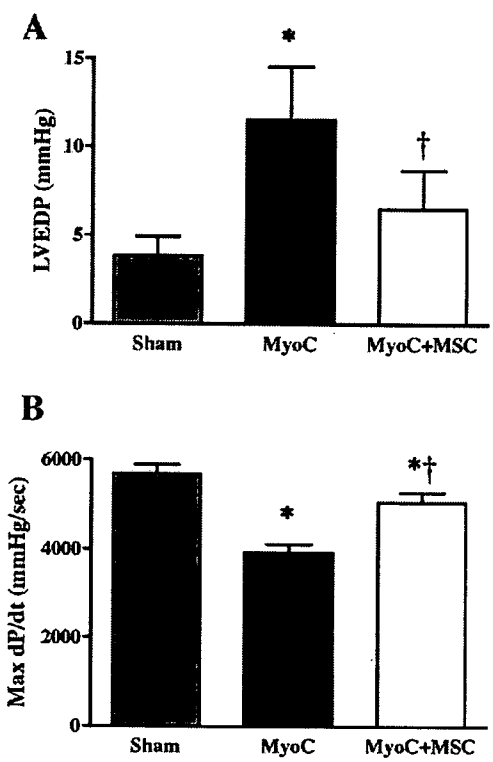

Fig. 1. Effects of MSC transplantation on hemodynamic parameters in acute myocarditis. (A) Left ventricular end-diastolic pressure (LVEDP) and (B) maximum dP/dt (Max dP/dt) were measured in sham-operated rats given vehicle (Sham group), myosin-treated rats given vehicle (MyoC group), and myosin-treated rats given MSC (MyoC+MSC group). Values are mean±S.E. *$P<0.05$ *vs* Sham, †$P<0.05$ *vs* MyoC group.

Table 1
Physiological parameters in three experimental groups

	Sham	MyoC	MyoC+MSC
HW/BW (g/kg)	2.9±0.3	6.4±0.3*	4.7±0.3*,†
HR (bpm)	446±11	363±14*	442±12*,†
MAP (mm Hg)	108±3	87±3*	108±4†
LVSP (mm Hg)	130±2	105±4*	125±4†
Min d*P*/d*t* (mm Hg/s)	−5440±199	−3097±183*	−4617±171*,†

Sham, sham-operated rats given vehicle; MyoC, myosin-treated rats given vehicle; MyoC+MSC, myosin-treated rats given MSC (3×10^6 cells); HW/BW, heart weight to body weight ratio; HR, heart rate; MAP, mean arterial pressure; LVSP, left ventricular systolic pressure; Mim d*P*/d*t*, minimum d*P*/d*t*. Data are mean±S.E. *$P<0.05$ *vs* Sham, †$P<0.05$ *vs* MyoC group.

instructions. The cells were then mounted in medium containing DAPI. Randomly selected microscopic fields ($n=5$) were evaluated to calculate the ratio of TUNEL-positive cells to total cells.

Table 2
Echocardiographic findings in three experimental groups

	Sham	MyoC	MyoC+MSC
LVDs (mm)	3.1±0.1	5.0±0.4*	3.8±0.2†
EF (%)	74.9±1.2	56.6±3.4*	71.2±3.5†
AWT diastole (mm)	1.9±0.1	3.0±0.2*	3.0±0.3*
PWT diastole (mm)	1.9±0.1	3.4±0.1*	2.7±0.2*,†

Sham, sham-operated rats given vehicle; MyoC, myosin-treated rats given vehicle; MyoC+MSC, myosin-treated rats given MSC (3×10^6 cells); LVDs, left ventricular systolic dimension; EF, ejection fraction; AWT, anterior wall thickness; PWT, posterior wall thickness. Data are mean±S.E. *$P<0.05$ *vs* Sham, †$P<0.05$ *vs* MyoC group.

2.13. Creatine kinase (CK) activity assay

CK activity in culture media was measured after incubation of cardiomyocytes for 24 h ($n=5$), using the enzyme measurement kit (Kanto Chemical, Tokyo, Japan).

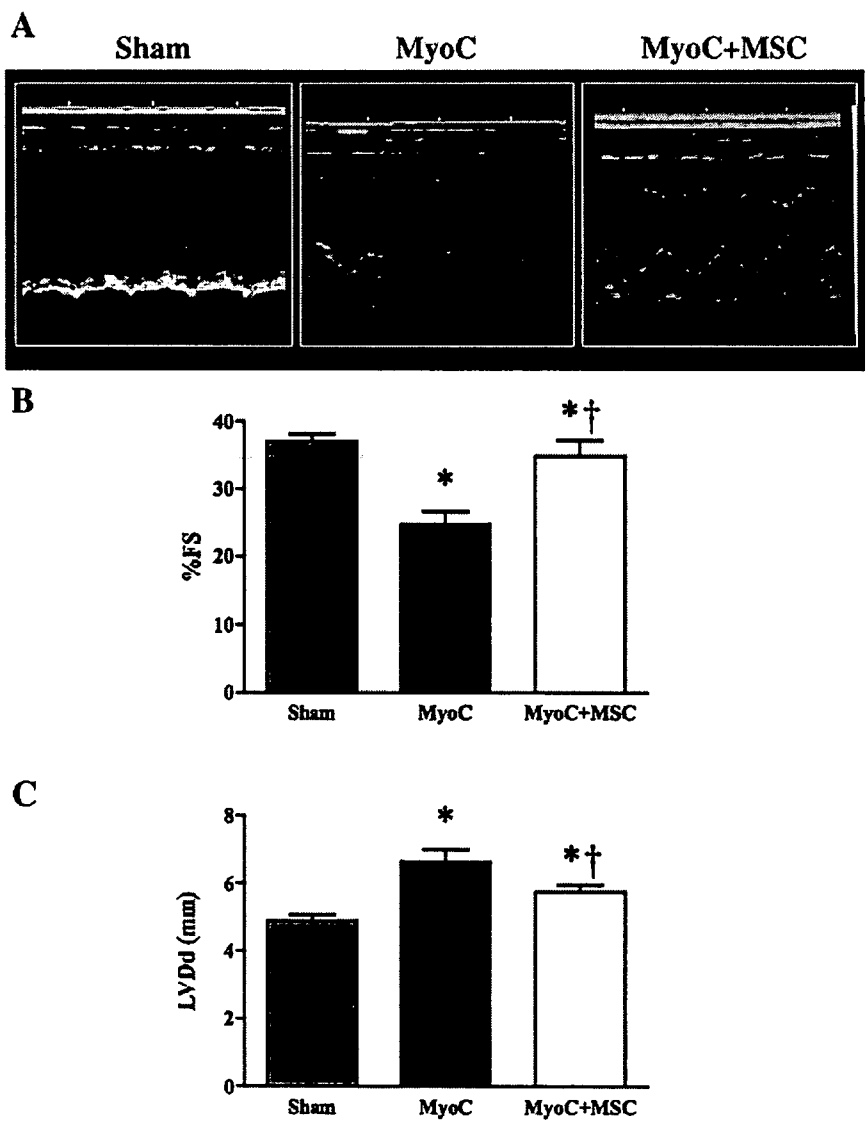

Fig. 2. Effects of MSC transplantation on echocardiographic parameters in acute myocarditis. (A) Representative echocardiographic images showing wall thickening and poor movement in the MyoC group, and improvement of cardiac contractility in the MyoC+MSC group. (B and C) MSC transplantation significantly improved

2.14. Statistical analysis

Data were expressed as mean ± standard error (S.E.). Comparisons of parameters among groups were made by one-way ANOVA, followed by Newman–Keuls' test. Differences were considered significant at $P<0.05$.

3. Results

3.1. Improvement in cardiac function by MSC transplantation

Two of 15 rats in the MyoC group died on day 19 and day 21 post-myosin injection, respectively, whereas the MyoC+MSC group had no mortality. At 3 weeks post-myosin injection, the MyoC group showed increased heart weight/body weight ratio (HW/BW) and LVEDP, and decreased MAP and Max d*P*/d*t* compared with the Sham group, indicating the presence of acute heart failure in this model (Fig. 1 and Table 1). These parameters subsequently returned to baseline with MSC transplantation (MyoC+MSC group). On echocardiography, the MyoC group showed an increase in LVDs and LVDd, and a significant reduction in %FS and EF (Fig. 2 and Table 2). MSC transplantation significantly improved these parameters (MyoC+MSC group).

3.2. Attenuation of myocardial inflammation by MSC transplantation

Myocardial necrosis and tissue granulation as well as giant cell infiltration and edema were markedly increased in our model of acute myocarditis (Fig. 3A). MSC transplantation significantly attenuated these changes observed in the MyoC group. MSC-transplanted hearts exhibited a consistent tendency for a reduction of tissue granulation, inflammation and edema, on blinded histological grading by a cardiovascular pathologist (H.I-U.), as compared to the MyoC group (Fig. 3B). Hearts showed limited fibrosis in the MyoC group, and this observation was not significantly attenuated by MSC

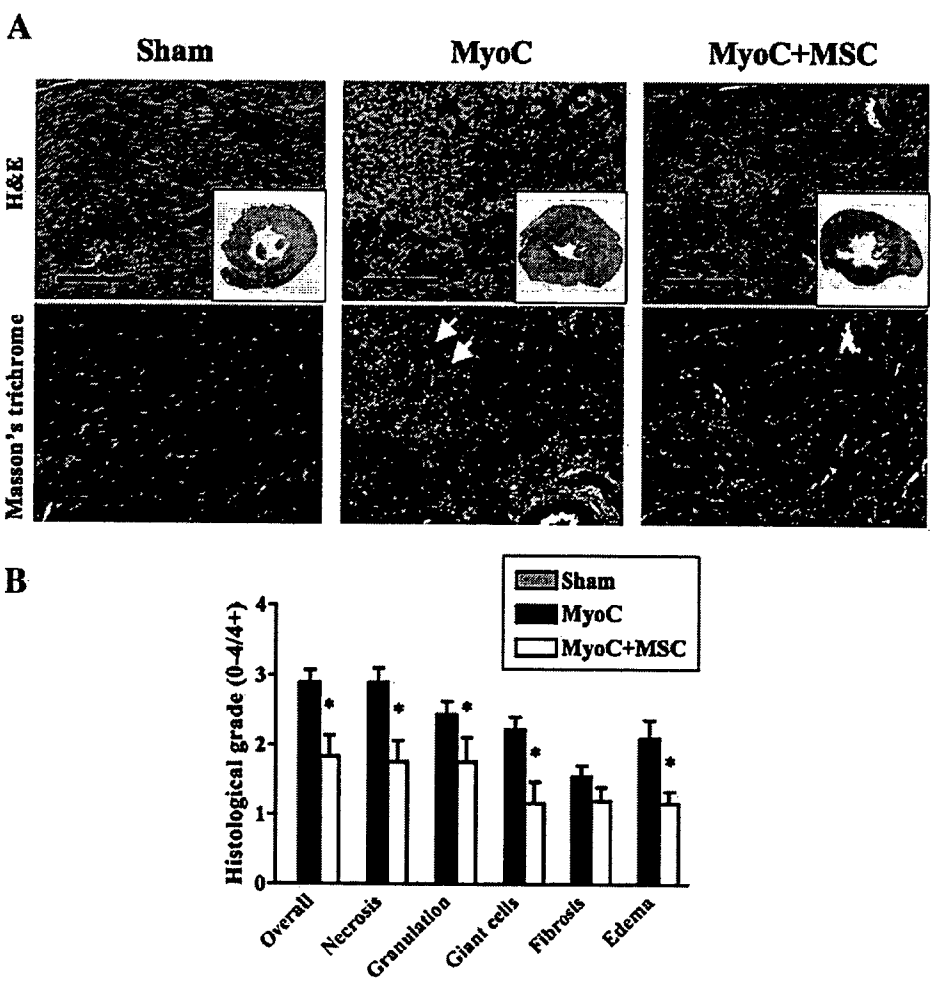

Fig. 3. Effects of MSC transplantation on pathological changes in acute myocarditis. (A) Representative myocardial sections show markedly decreased inflammation and tissue necrosis (H & E) and a comparable degree of early fibrosis (Masson's trichrome) after MSC transplantation (MyoC+MSC) as compared to control (MyoC, arrows). Insets are transverse sections of myocardium. Scale bars: 50 μm. (B) Semi-quantitative histological grades for necrosis and tissue granulation as well as for infiltration of giant cells and edema were significantly lower after MSC transplantation (MyoC+MSC) compared to control (MyoC). Sham tissues exhibited no measurable pathological change. Values are mean±S.E. *$P<0.05$ *vs* Sham, †$P<0.05$ *vs* MyoC group.

transplantation, possibly because of the acute nature of this experiment (Fig. 3B).

Notably, marked histiocytic infiltration was demonstrated by CD68-positive cells, including multinucleated giant cells, in myocarditis (MyoC group), and this was significantly attenuated by MSC transplantation (Figs. 4A and B). In myocarditis, there was an increase in MCP-1 expression localized to the vascular endothelium and also in cardiomyocytes surrounding areas of inflammation (Fig. 5A). The hearts in the MyoC+MSC group showed a partial decrease in MCP-1 expression. Serum MCP-1 level was greatly increased in the MyoC group, whereas the increase was significantly attenuated in the MyoC+MSC group (Fig. 5B).

3.3. Effect of MSC on angiogenesis

To investigate the angiogenic effect of MSC transplantation in the myocardium, immunohistochemical analysis of vWF was performed. Capillary density was increased in the MyoC group (Figs. 6A and B). Notably, in MSC-transplanted tissues, capillary density was increased compared to that in the MyoC group. The clustering of relatively small vessels seen in MSC-transplanted hearts was indicative of recent neovascularization.

3.4. Cardioprotective effects of MSC in paracrine manner

Because MSC transplantation had anti-inflammatory and tissue-protective effects and induced angiogenesis, some paracrine effects were expected. To confirm the paracrine effects of MSC *in vitro*, cardiomycytes were isolated from adult rats, and cultured with MCP-1 in the standard medium or in the conditioned medium obtained from MSC culture. The standard medium containing MCP-1 resulted in a decrease in viable cardiomyocytes; however, MSC-derived conditioned medium containing MCP-1 attenuated the decrease in viable cardiomyocytes (Fig. 7A). TUNEL staining showed that the standard medium containing MCP-1 markedly induced apoptosis of cardiomyocytes (Figs. 7B and C). However, the conditioned medium of MSC significantly attenuated MCP-1-induced cardiomyocyte apoptosis. In addition, CK activity in standard medium containing MCP-1 was significantly increased, whereas the conditioned medium markedly attenuated the CK activity induced by MCP-1 (Fig. 7D).

To investigate whether MSC secreted angiogenic and anti-fibrotic factors, VEGF and HGF levels in MSC culture were measured by ELISA assay. MSC secreted large amounts of VEGF and HGF compared to standard medium, respectively (Fig. 7E).

4. Discussion

In this study, we focused on the therapeutic potential of MSC transplantation in the acute phase of myocarditis. We showed that 1) MSC transplantation 1 week after myosin injection improved cardiac function and attenuated pathological findings including myocardial inflammation, and that 2)

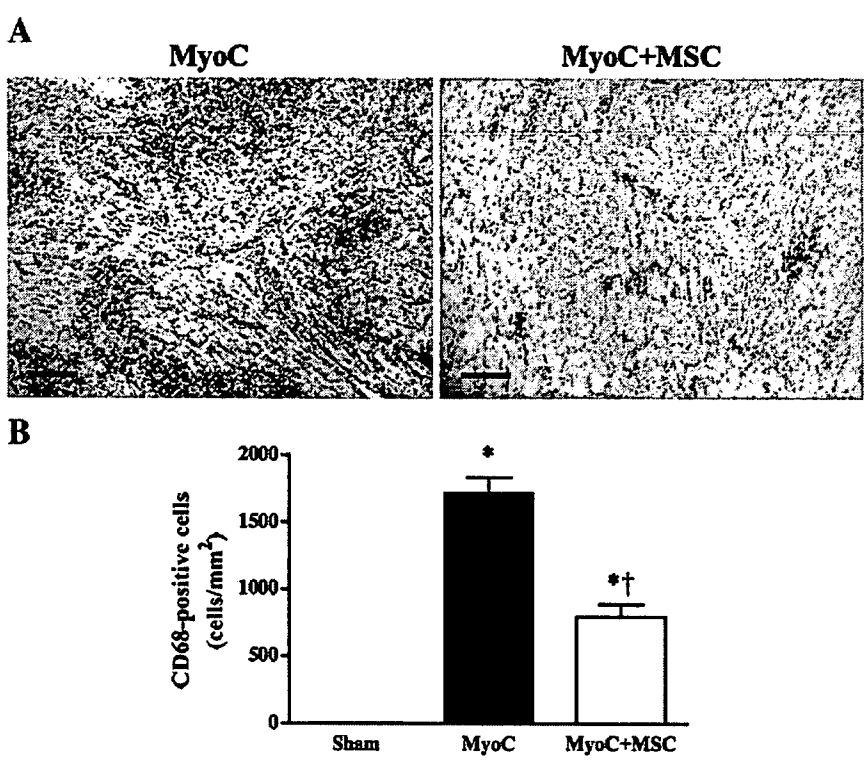

Fig. 4. Effects of MSC transplantation on myocardial CD68 expression in acute myocarditis. (A) Representative myocardial sections immunohistochemically stained for CD68 demonstrate a marked decrease in CD68-positive cells, including giant cells, after MSC transplantation (MyoC+MSC) as compared to control (MyoC). Scale bars: 100 μm. (B) Semi-quantitative counts of CD68-positive cells demonstrate a significant reduction in the MyoC+MSC group. Values are mean±S.E. *$P<0.05$ *vs* Sham, †$P<0.05$ *vs* MyoC group.

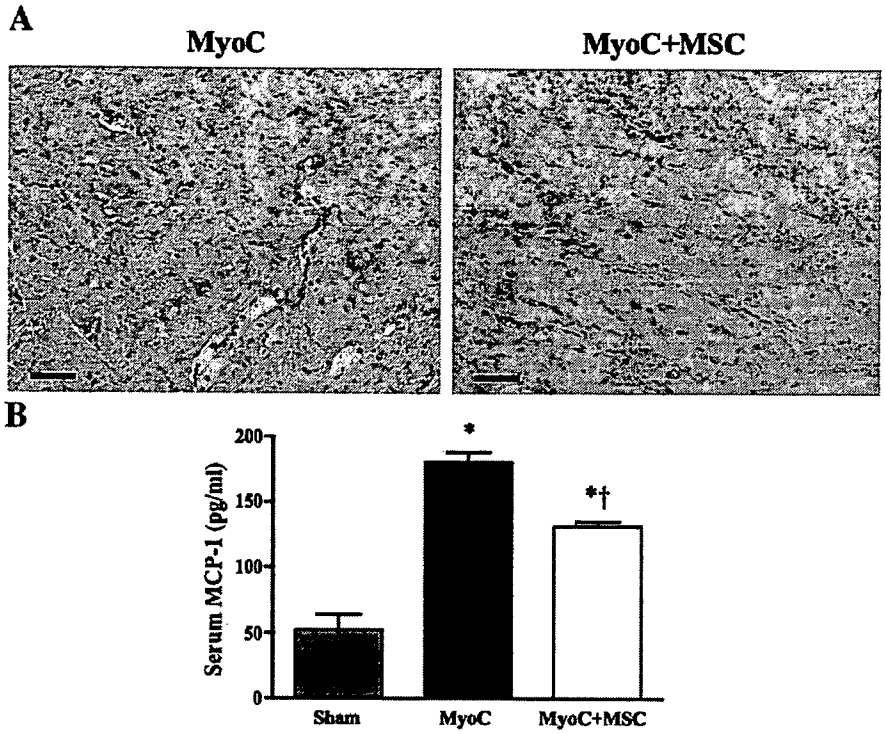

Fig. 5. Effects of MSC transplantation on myocardial MCP-1 expression and serum MCP-1 level. (A) Representative MCP-1-stained myocardial sections from MyoC and MyoC+MSC groups. Scale bars: 50 μm. (B) Serum level of MCP-1 measured by ELISA. Values are mean±S.E. *$P<0.05$ *vs* Sham, †$P<0.05$ *vs* MyoC group.

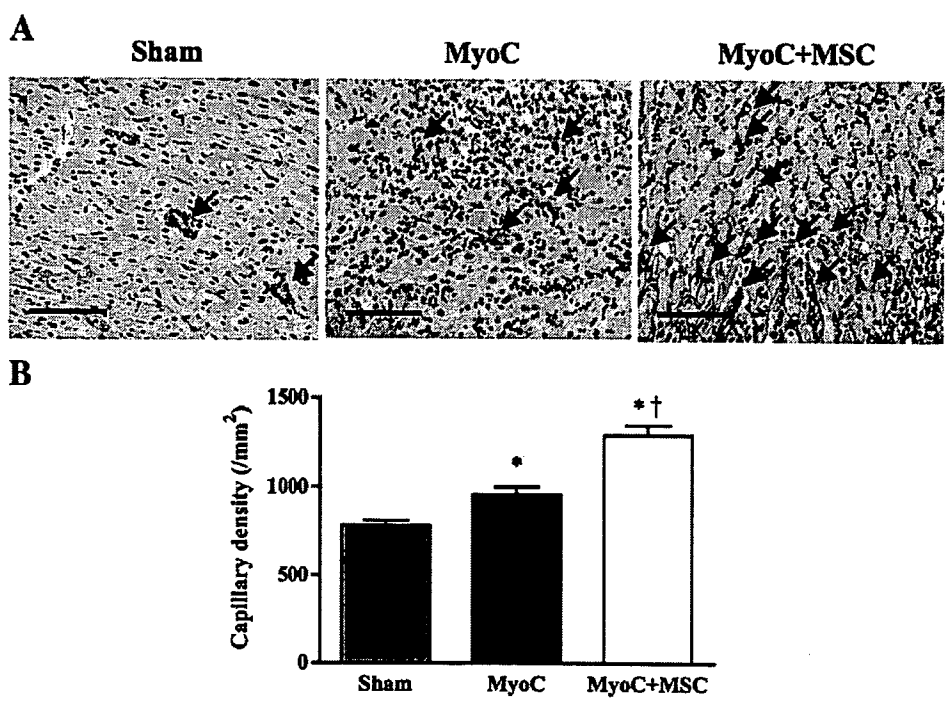

Fig. 6. Effects of MSC on neovascularization. (A) Representative myocardial sections immunohistochemically stained for vWF showing increased microvasculature (arrows) in control hearts (MyoC), which was more marked after MSC transplantation (MyoC+MSC). Scale bars: 50 μm. (B) Capillary density measured in 10 random representative high-power fields showing a significant increase in control (MyoC) and a further increase after MSC transplantation (MyoC+MSC) over the Sham group. Values are mean±S.E. *$P<0.05$ *vs* Sham, †$P<0.05$ *vs* MyoC group.

MSC had cardioprotective effects acting in a paracrine manner.

The rat model of myosin-induced experimental myocarditis provides a model that resembles human giant cell myocarditis [8,10]. Although the majority of acute myocarditis is linked to a viral infection such as coxsackievirus B3, this viral infection can in some cases cause an autoimmune myocarditis with chronic myocardial inflammation without viral persistence, due to the exposure of cardiac autoantigens to the immune system [11,12]. This myocarditis model is triphasic, consisting of an antigen priming phase from days 0–14, an autoimmune response phase from days 14–21, and a reparative phase thereafter, associated chronically with a dilated cardiomyopathy phenotype [13]. In our previous study, MSC were transplanted at the reparative

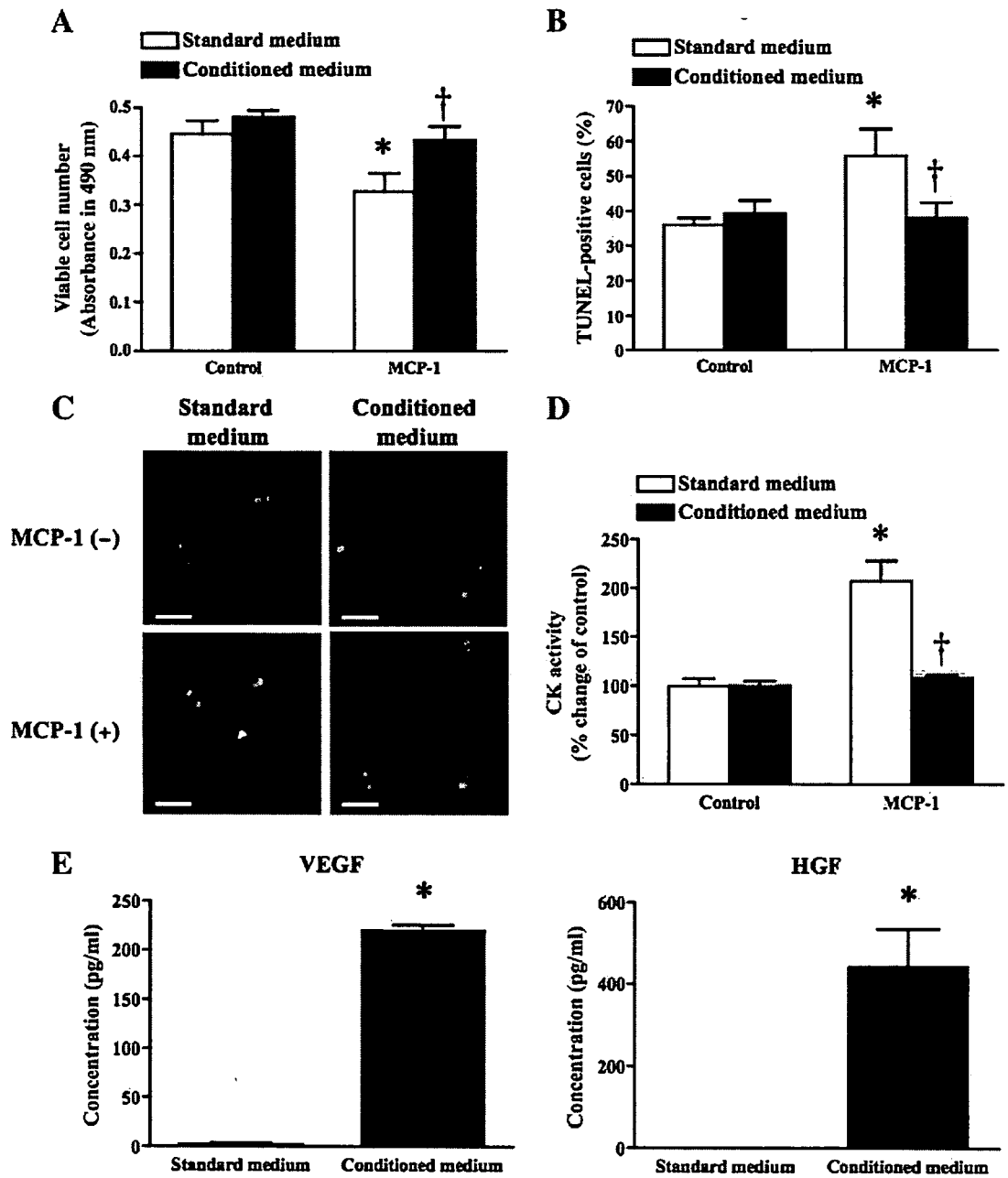

Fig. 7. Effects of MSC on MCP-1-induced cardiomyocyte injury *in vitro*. (A) MTS assay after 24 h of culture with or without MCP-1 in standard medium *vs* MSC conditioned medium. *$P<0.05$ *vs* control in standard medium, †$P<0.05$ *vs* MCP-1 in conditioned medium. (B) Quantitative analysis of TUNEL staining after 24 h of culture with or without MCP-1 in standard medium *vs* MSC conditioned medium. *$P<0.05$ *vs* control in standard medium, †$P<0.05$ *vs* MCP-1 in standard medium. (C) Representative TUNEL staining show increased apoptotic cardiomyocytes (green) cultured with MCP-1 in standard medium, which was attenuated by MSC conditioned medium. Nuclei were counterstained with DAPI (blue). Scale bars: 50 μm. (D) CK activity after 24 h of culture with or without MCP-1 in standard medium *vs* MSC conditioned medium. *$P<0.05$ *vs* control in standard medium, †$P<0.05$ *vs* MCP-1 in standard medium. (E) ELISA for VEGF and HGF secreted from cultured MSC as compared to standard medium. †$P<0.05$ *vs* standard medium.

phase with a dilated cardiomyopathy phenotype, by direct injection into the myocardium [7]. In the present study, however, MSC were transplanted 1 week following myosin injection, corresponding to the acute phase of myocarditis, by intravenous injection, because this model is more relevant to clinical situations. Myosin injection caused acute heart failure as indicated by increased LVEDP and decreased Max dP/dt and %FS, and 2 out of 15 rats died; however, intravenous injection of MSC in the acute phase significantly improved the heart failure as determined by improvement of these parameters, and no death was observed.

Wang et al. have shown that embryonic stem (ES) cells transplanted into a mouse model of myocarditis regenerate cardiomyocytes, decrease inflammation and increase survival, possibly through migration of ES cells and differentiation into cardiomyocytes [14]. In the present study, we examined the therapeutic potential of transplanted MSC, which are more applicable to clinical situations than ES cells, in a rat model of acute myocarditis. Recent studies have demonstrated that autologous or allogeneic MSC strongly suppress T-lymphocyte proliferation [15,16]. These findings raise the possibility that MSC have the ability to attenuate inflammatory responses. Interestingly, the present study demonstrated that transplantation of MSC attenuated the infiltration of CD68-positive inflammatory cells and the expression of MCP-1 in a rat model of acute myocarditis. MCP-1 is a member of the C–C subfamily of chemokines with chemoattractant activity for major inflammatory cells, and is known to play an important role in the induction of experimental acute myocarditis [17,18]. Cardiac-targeted expression of MCP-1 results in monocyte/macrophage infiltration into the heart, and causes interstitial fibrosis and ventricular chamber dilation [19]. In the myosin-induced acute myocarditis model, MCP-1 expression is increased in the heart from days 15–27 post-myosin injection, and serum MCP-1 level is elevated from days 15–24 [18]. In consistent with this report, our model showed an increase in MCP-1 in the heart and serum on day 21 post-myosin injection, and MSC transplantation attenuated the increase in MCP-1 and the infiltration of CD68-positive inflammatory cells. Furthermore, earlier studies have shown that MSC express CCR2, the receptor for MCP-1, and that MCP-1 promotes the migration of MSC that express CCR2 [20,21]. Thus, it is speculated that MSC secrete some anti-inflammatory factors in response to MCP-1; however, the precise mechanisms for the anti-inflammatory effect still remains to be elucidated.

Because MCP-1 plays an important role in this myosin-induced myocarditis model, we examined the direct effect of MCP-1, besides its chemoattractant activity, on adult rat cardiomyocytes. Our *in vitro* experiment demonstrated that MCP-1 stimulation on cardiomyocytes resulted in an increase of cell injury and death, whereas MSC-derived conditioned medium attenuated these effects. It has been reported that CCR2 expression is increased in the failing myocardium, and MCP-1 stimulation on cardiomyocytes induces other inflammatory cytokines such as IL-1β and IL-6, which may reduce cardiomyocyte contractility partly via induction of apoptosis [22–25]. In addition, our previous and present study demonstrated that cultured MSC secreted large amounts of angiogenic and anti-apoptotic factors such as VEGF, HGF, insulin-like growth factor-1 and adrenomedullin [7]. Furthermore, a recent study demonstrated that conditioned medium obtained from MSC culture had cardioprotective effect [26]. Taken together, although various factors might be involved, MSC might have cardioprotective effects in a paracrine manner in response to MCP-1.

In the present study, MSC transplantation increased capillary density in the myocardium. Improvement in myocardial vascular supply has been shown to decrease necrosis and inflammation in viral myocarditis [8,27,28]. We have previously reported increased capillary density associated with improved cardiac function and decreased infarct size following MSC transplantation in a rat model of myocardial infarction [5]. These results suggest that MSC-induced neovascularization may have contributed to the improvement of cardiac function in this rat model of acute myocarditis. However, when PKH26 dye-labeled MSC were intravenously injected in rats with acute myocarditis, only a small fraction of PKH26-labeled cells were positive for troponin T 2 weeks after transplantation (data not shown). Our previous study demonstrated that ~3% of the intravenously administered MSCs were incorporated into the heart 24 h after transplantation in rats with acute myocardial infarction [5]. Although the animal model and the evaluation time were different, our present study showed that only a small number of administered MSC was differentiated into endothelial cells or cardiomyocytes, thus the contribution of the differentiated MSC to the improvement of cardiac function in this model appears to be rather insignificant.

In conclusion, MSC transplantation attenuated myocardial injury and dysfunction in a rat model of acute myocarditis, at least in part through paracrine effects of MSC.

Acknowledgments

This work was funded by a post-doctoral fellowship from the Japan Society for the Promotion of Science, and research grants for Cardiovascular Disease (16C-6, 17C-1 and 18C-1) and Human Genome Tissue Engineering 009 from the Ministry of Health, Labor and Welfare.

References

[1] Levi D, Alejos J. Diagnosis and treatment of pediatric viral myocarditis. Curr Opin Cardiol 2001;16:77–83.
[2] Feldman AM, McNamara D. Myocarditis. N Engl J Med 2000;343:1388–98.
[3] Pittenger MF, Mackay AM, Beck SC, Jaiswal RK, Douglas R, Mosca JD, et al. Multilineage potential of adult human mesenchymal stem cells. Science 1999;284:143–7.
[4] Le Blanc K, Pittenger M. Mesenchymal stem cells: progress toward promise. Cytotherapy 2005;7:36–45.
[5] Nagaya N, Fujii T, Iwase T, Ohgushi H, Itoh T, Uematsu M, et al. Intravenous administration of mesenchymal stem cells improves cardiac function in rats with acute myocardial infarction through angiogenesis and myogenesis. Am J Physiol: Heart Circ Physiol 2004;287:H2670–6.

[6] Miyahara Y, Nagaya N, Kataoka M, Yanagawa B, Tanaka K, Hao H, et al. Monolayered mesenchymal stem cells repair scarred myocardium after myocardial infarction. Nat Med 2006;12:459–65.
[7] Nagaya N, Kangawa K, Itoh T, Iwase T, Murakami S, Miyahara Y, et al. Transplantation of mesenchymal stem cells improves cardiac function in a rat model of dilated cardiomyopathy. Circulation 2005; 112:1128–35.
[8] Kodama M, Matsumoto Y, Fujiwara M, Masani F, Izumi T, Shibata A. A novel experimental model of giant cell myocarditis induced in rats by immunization with cardiac myosin fraction. Clin Immunol Immunopathol 1990;57:250–62.
[9] Tanaka K, Honda M, Takabatake T. Redox regulation of MAPK pathways and cardiac hypertrophy in adult rat cardiac myocyte. J Am Coll Cardiol 2001;37:676–85.
[10] Kodama M, Matsumoto Y, Fujiwara M, Zhang SS, Hanawa H, Itoh E, et al. Characteristics of giant cells and factors related to the formation of giant cells in myocarditis. Circ Res 1991;69:1042–50.
[11] Fairweather D, Kaya Z, Shellam GR, Lawson CM, Rose NR. From infection to autoimmunity. J Autoimmun 2001;16:175–86.
[12] Cunningham MW. T cell mimicry in inflammatory heart disease. Mol Immunol 2004;40:1121–7.
[13] Kodama M, Hanawa H, Saeki M, Hosono H, Inomata T, Suzuki K, et al. Rat dilated cardiomyopathy after autoimmune giant cell myocarditis. Circ Res 1994;75:278–84.
[14] Wang JF, Yang Y, Wang G, Min J, Sullivan MF, Ping P, et al. Embryonic stem cells attenuate viral myocarditis in murine model. Cell Transplant 2002;11:753–8.
[15] Di Nicola M, Carlo-Stella C, Magni M, Milanesi M, Longoni PD, Matteucci P, et al. Human bone marrow stromal cells suppress T-lymphocyte proliferation induced by cellular or nonspecific mitogenic stimuli. Blood 2002;99: 3838–43.
[16] Tse WT, Pendleton JD, Beyer WM, Egalka MC, Guinan EC. Suppression of allogeneic T-cell proliferation by human marrow stromal cells: implications in transplantation. Transplantation 2003;75:389–97.
[17] Rollins BJ. Chemokines. Blood 1997;90:909–28.
[18] Fuse K, Kodama M, Hanawa H, Okura Y, Ito M, Shiono T, et al. Enhanced expression and production of monocyte chemoattractant protein-1 in myocarditis. Clin Exp Immunol 2001;124:346–52.
[19] Kolattukudy PE, Quach T, Bergese S, Breckenridge S, Hensley J, Altschuld R, et al. Myocarditis induced by targeted expression of the MCP-1 gene in murine cardiac muscle. Am J Pathol 1998;152:101–11.
[20] Ji JF, He BP, Dheen ST, Tay SS. Interactions of chemokines and chemokine receptors mediate the migration of mesenchymal stem cells to the impaired site in the brain after hypoglossal nerve injury. Stem Cells 2004;22:415–27.
[21] Wang L, Li Y, Chen J, Gautam SC, Zhang Z, Lu M, et al. Ischemic cerebral tissue and MCP-1 enhance rat bone marrow stromal cell migration in interface culture. Exp Hematol 2002;30:831–6.
[22] Damas JK, Eiken HG, Oie E, Bjerkeli V, Yndestad A, Ueland T, et al. Myocardial expression of CC- and CXC-chemokines and their receptors in human end-stage heart failure. Cardiovasc Res 2000;47:778–87.
[23] Damas JK, Aukrust P, Ueland T, Odegaard A, Eiken HG, Gullestad L, et al. Monocyte chemoattractant protein-1 enhances and interleukin-10 suppresses the production of inflammatory cytokines in adult rat cardiomyocytes. Basic Res Cardiol 2001;96:345–52.
[24] Ing DJ, Zang J, Dzau VJ, Webster KA, Bishopric NH. Modulation of cytokine-induced cardiac myocyte apoptosis by nitric oxide, Bak, and Bcl-x. Circ Res 1999;84:21–33.
[25] Hirota H, Chen J, Betz UA, Rajewsky K, Gu Y, Ross Jr J, et al. Loss of a gp130 cardiac muscle cell survival pathway is a critical event in the onset of heart failure during biomechanical stress. Cell 1999;97: 189–98.
[26] Gnecchi M, He H, Liang OD, Melo LG, Morello F, Mu H, et al. Paracrine action accounts for marked protection of ischemic heart by Akt-modified mesenchymal stem cells. Nat Med 2005;11:367–8.
[27] Lee JK, Zaidi SH, Liu P, Dawood F, Cheah AY, Wen WH, et al. A serine elastase inhibitor reduces inflammation and fibrosis and preserves cardiac function after experimentally-induced murine myocarditis. Nat Med 1998;4:1383–91.
[28] Ono K, Matsumori A, Shioi T, Furukawa Y, Sasayama S. Contribution of endothelin-1 to myocardial injury in a murine model of myocarditis: acute effects of bosentan, an endothelin receptor antagonist. Circulation 1999;100:1823–9.